Science Advances
AAAS

Supplementary Materials for

Interactive nanocluster compaction of the ELKS scaffold and Cacophony Ca^{2+} channels drives sustained active zone potentiation

Tina Ghelani *et al.*

Corresponding author: Martin Heine, marthein@uni-mainz.de; Stephan J. Sigrist, stephan.sigrist@fu-berlin.de

Sci. Adv. **9**, eade7804 (2023)
DOI: 10.1126/sciadv.ade7804

The PDF file includes:

Other Supplementary Material for this manuscript includes the following:

Supplemental Figures and Supplemental Figure legends for movies:

Live *in vivo* localization microscopy (sptPALM) of CacmEOS4b molecules

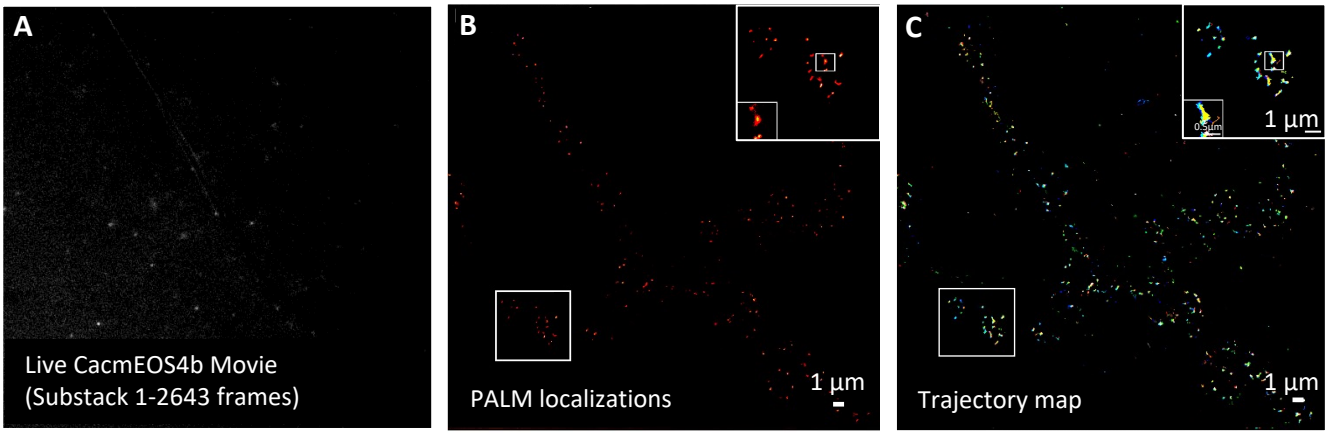

Localization accuracy and photon counts of CacmEOS4b molecules

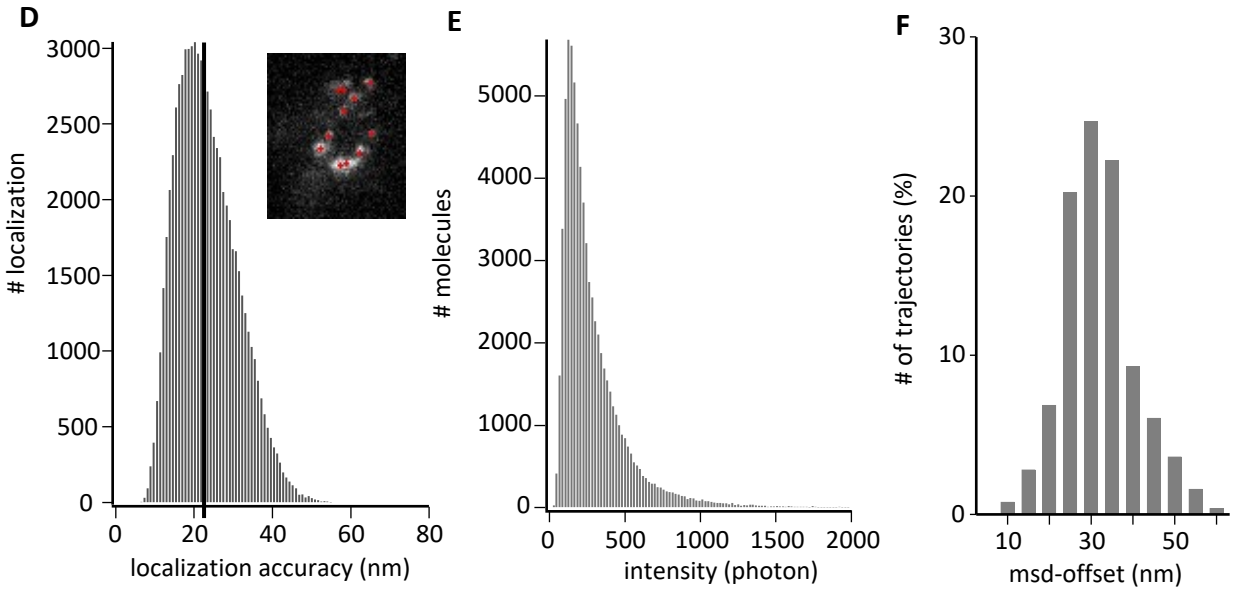

Figure S1. Parameters of single molecule localization microscopy experiments in *Drosophila* larvae.
(A-C) Representative movie of an entire *Drosophila* Muscle 6 NMJ imaged live, in vivo with sptPALM for 5000 frames at 20 Hz frame rate (1-2643 frames shown) can be seen in Supplemental Movie 1. From this movie (A), the PALM localization map (B) and trajectory map (C) was derived for analysis. Scale Bars (B-C) =1 µm and inset (C) 0.5 µm. (D) Localization accuracy of individual events (n=72713) within 6 presynaptic boutons from 6 animals recorded for 2500-5000 frames. The mean localization accuracy is 23.7 ± 7.7 nm (median 22.7 nm IQR 17.8 nm / 28.7 nm). Insert shows single frame image of a bouton and the detected molecule localization (red crosses). (E) Intensity distribution of detected molecules, mean photon count for individual mEOS4b tagged channels was 297.3 ± 227.9 photons (median 227.3 IQR 152.7 / 364.1) from same experiments as in (E). (F) Trajectories from immobile/confined molecules that resulted in MSD-curves parallel to the x-axis of the MSD versus time plot (Fig.1O) were taken as independent controls for the localization accuracy within sptPALM experiments after reconstruction of individual trajectories, here only trajectories longer than 10 points were included. The average offset of the immobilized MSD plot was 31.3 nm IQR 25.9 / 36.6 nm. The viability of *Drosophila* larvae filet preparation within the imaging experiment was tested by prolonged imaging of individual NMJs. The frequency of spontaneous activity was monitored by calcium imaging of postsynaptic events in animals expressing the calcium sensor Syn-GCamp6f within the muscular membrane and the CacmEOS4b within the presynaptic bouton.

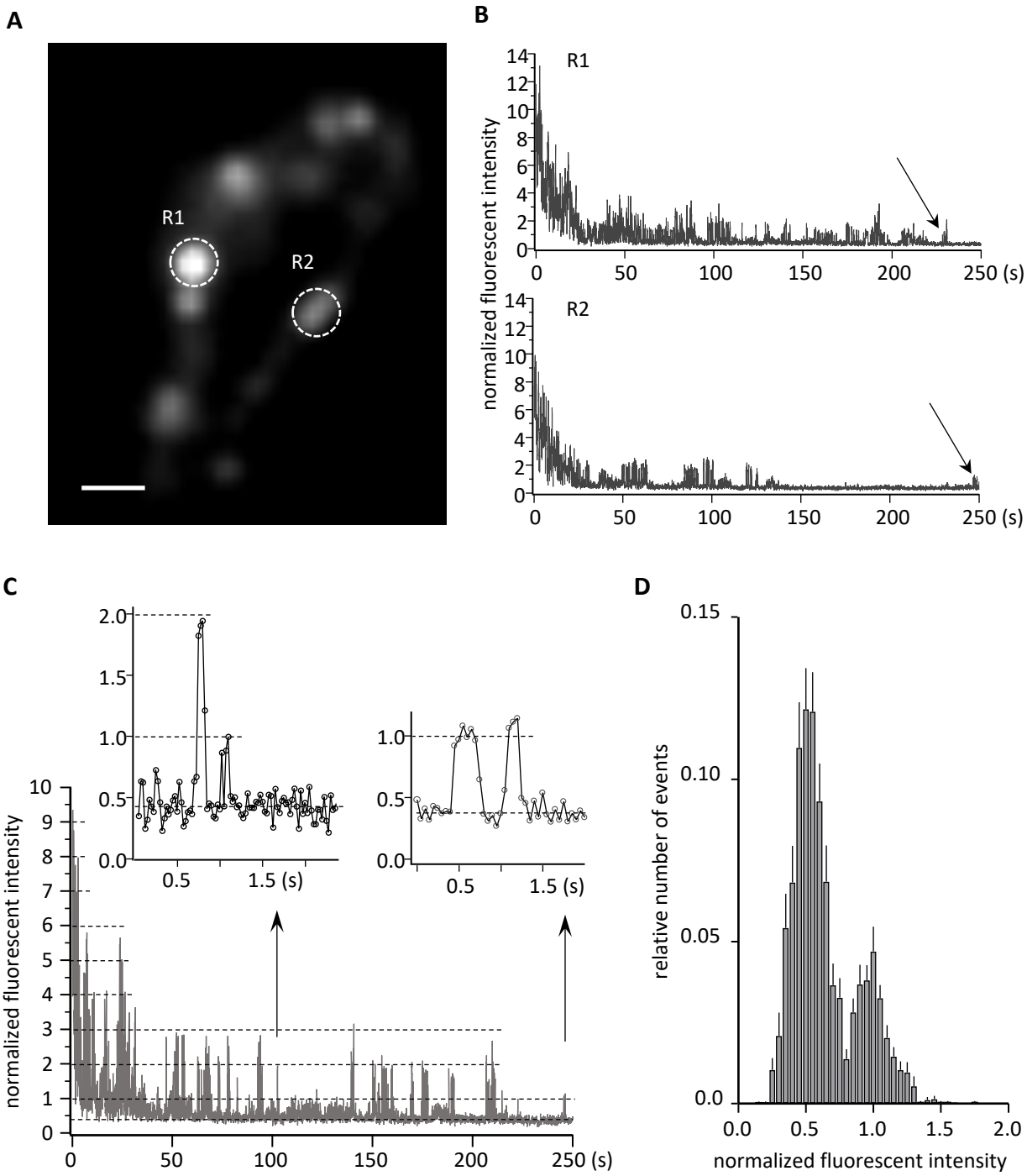

Figure S2. Parameters of bleach curve analysis from sptPALM live imaging experiments in *Drosophila* larvae.
Estimation of relative channel numbers based on the blinking fluorescent emission of mEOS4b tagged cacophony channels. (A) Averaged fluorescent intensity of a bouton recorded for 250 s, indicated are the analyzed regions, scale bar 1 µm. (B) Fluorescent intensity measurements over time, normalized first to the average background signal and second to the average amplitude of single fluorophore events at the end of the recording as indicated (arrow). (C) Similar fluorescent intensity profile after dual normalization. The estimate of the single fluorescent events had to be made for each record individually, due to local changes of fluorescence in the preparation. Note the slight drift of the baseline due to ongoing photo bleach, which biased the accuracy of the maximal channel number. (D) Averaged distribution of single fluorescent events in respect to the background after normalization. Data in (D) are from 24 active zones out of 5 control preparations (animals).

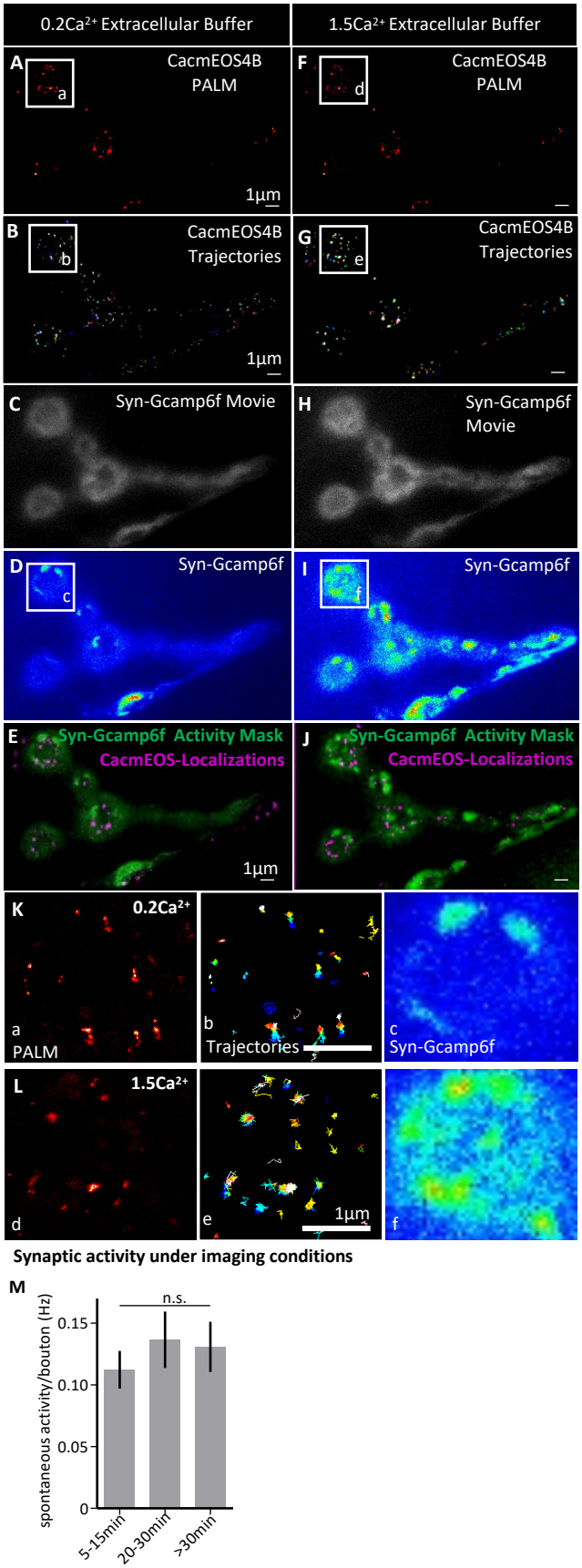

Figure S3. Parameters of single molecule localization microscopy experiments in *Drosophila* larvae. (A-J) live imaging of third-instar larvae at muscle 4 of *CacmEOS4b;;Syn-GCAMP6f* was first performed in low calcium (0.2 mM Ca^{2+}) (A-E) and then in control (1.5 mM Ca^{2+}) (F-J) extracellular imaging solution. Here, a live Syn-GCAMP6f recording was performed for 5000 frames at 50 Hz (C-E and H-J) presented in Supplemental Movie 2 and 3 respectively and is further followed by a sptPALM recording of CacmEOS4b performed at 20 Hz for 5000 frames (A-B and F-G). Accumulated activity masks of (C) or (H) derived from Supplemental Movie 2 and 3 respectively, are shown in (D) and (E), or (J) and (I), respectively. sptPALM image processing was applied to retrieve the PALM localizations and trajectories of Cac channels (A, B, F and G). (K-M) Zoomed insets (a-f) are represented in (K, Land M) The vitality of larval body wall preparations in sptPALM experiments was evaluated by monitoring spontaneous activity in 1.5 mM Ca^{2+} by postsynaptic Syn-GCamp6f. Repetitive recordings from individual NMJs over time resulted in a decay of spontaneous activity within 30 min. Imaging of different NMJ from different muscles did not result in a decay of spontaneous activity (M). For spontaneous activity measurements per bouton in 1.5 mM Ca^{2+} extracellular imaging solution, no significant change in spontaneous activity was found over 30 min of recordings. Data are from 4 animals per condition from which 19 boutons for alternated illumination were analyzed. Differences were tested by one way ANOVA followed by a Newman-Keul's multiple comparison test. Statistical significance is denoted as asterisks ***$p < 0.001$. Scale bars: 1µm.

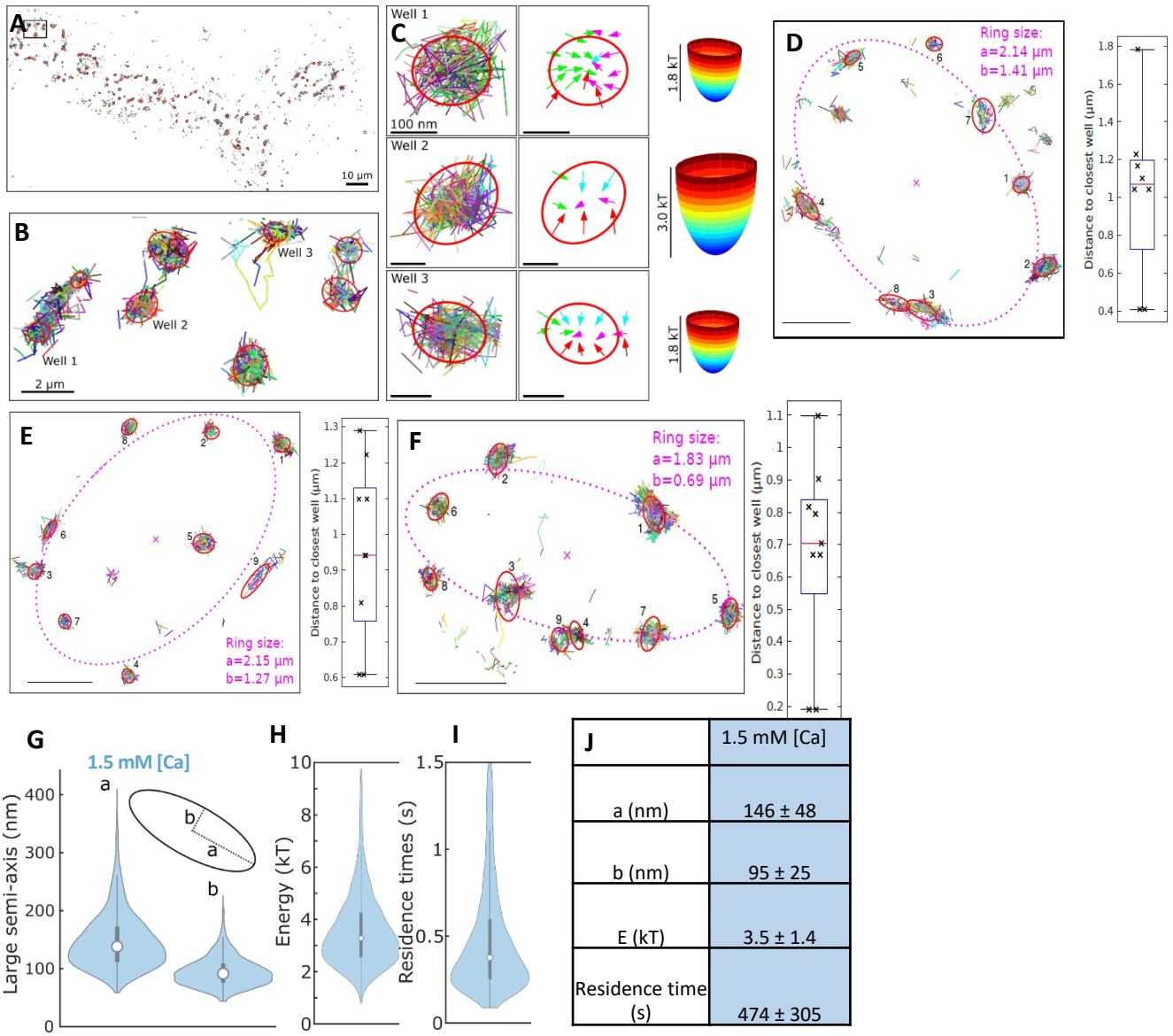

J	1.5 mM [Ca]
a (nm)	146 ± 48
b (nm)	95 ± 25
E (kT)	3.5 ± 1.4
Residence time (s)	474 ± 305

Figure S4. In well analysis of live *in vivo* mobility of individual voltage VGCCs at *Drosophila* NMJ synapses. (A) Single-particle trajectories of a representative NMJ displaying live Cac channel dynamics in third instar CacmEOS4B larvae localized at AZs. (B) Blow-up of the region shown in (A) and possessing multiple wells. (C) Three examples of wells showing retained trajectories (left), their corresponding drift fields (middle) and energy representations (right). (D-F) Three regions showing wells organised in rings. (G-I) Cac well analysis of well semi-axes lengths; (a: 146 ± 48 nm, b: 95 ± 25 nm) (G), within well energy (H), and within well Cac channel residence time (I). (J) a detailed list of averages of within well characteristics N=50 images from 15 animals from which 2041 wells analysed. Single Particle Trajectory maps of Individual *Drosophila* NMJ boutons presenting endogenous CacmEOS4b wells imaged under control extracellular 1.5 mM Ca^{2+} conditions display an inter-well distance of about 0.8 µm.

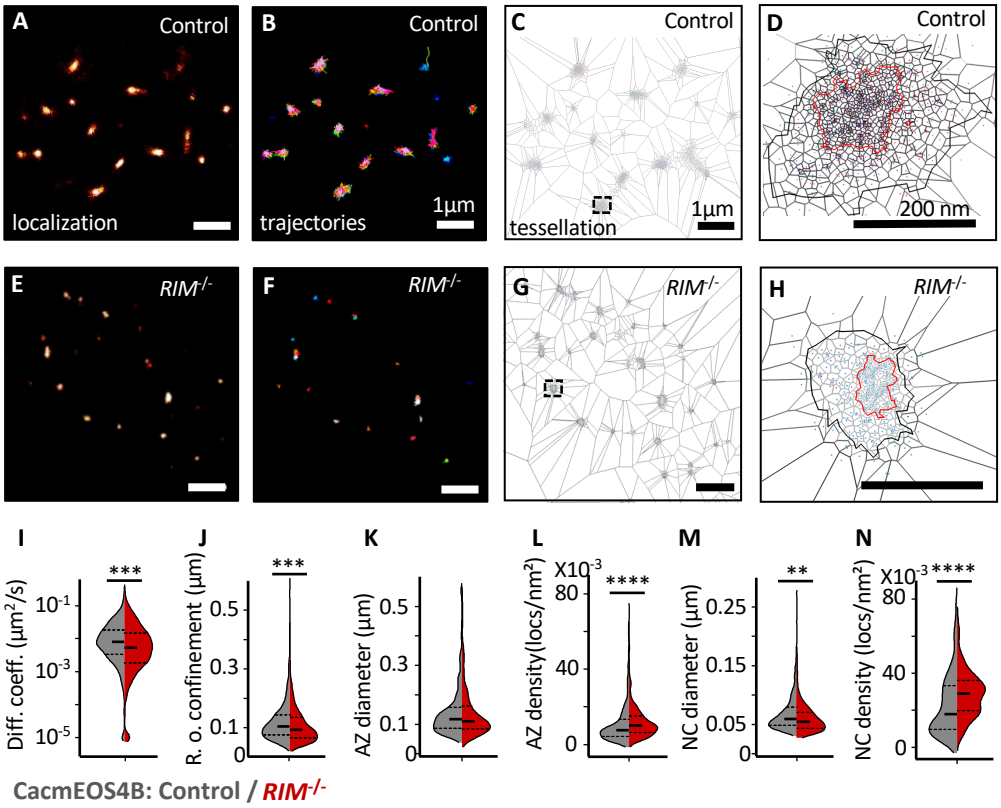

Figure S5. Cac channels in *RIM-1* mutant AZs channel visualized for their live mobility and distribution at AZs. Live sptPALM imaging of *CacmEOS4B* (Control) and *CacmEOS4B;;RIM-1*$^{-/-}$ (*RIM*$^{-/-}$) mutants imaged in 1.5mM Ca^{2+} extracellular imaging buffer. Representative boutons displaying PALM images (A, E), trajectory maps (B-F) and representation of tessellation analysis (C-D, G-H) of individual Cac channels in a bouton of *CacmEOS4B* (control) and *CacmEOS4B;;RIM*$^{-/-}$ animals. Scale bar: (A-C, E-G): 1 µm; (D, H): 200 nm. (I-J), live sptPALM diffusion coefficient and radius of confinement quantification of *CacmEOS4B* and *CacmEOS4B;;RIM*$^{-/-}$ NMJs, N=31 (Con) and 24 (*RIM*$^{-/-}$) ROIs from 12 and 8 animals respectively from which 2192 (Con) and 1644 (*RIM*$^{-/-}$) trajectories were analyzed. (K-N) Tessellation analysis of the diameter and density of Cac channels localizations within Nanocluster (NC) (M-N) and Active Zone (AZ) (K-L) boundaries from the same data as in I-J yielded 371 (Con) and 505 (*RIM*$^{-/-}$) AZs that were analyzed. n=3 individual *RIM*$^{-/-}$ experiments were conducted with concurrent controls. PALM Data distribution was statistically tested with Kolmogorov-Smirnov test. Statistical significance is denoted as asterisks: *p < 0.05; **p < 0.01; ***p < 0.001; ****p < 0.0001.

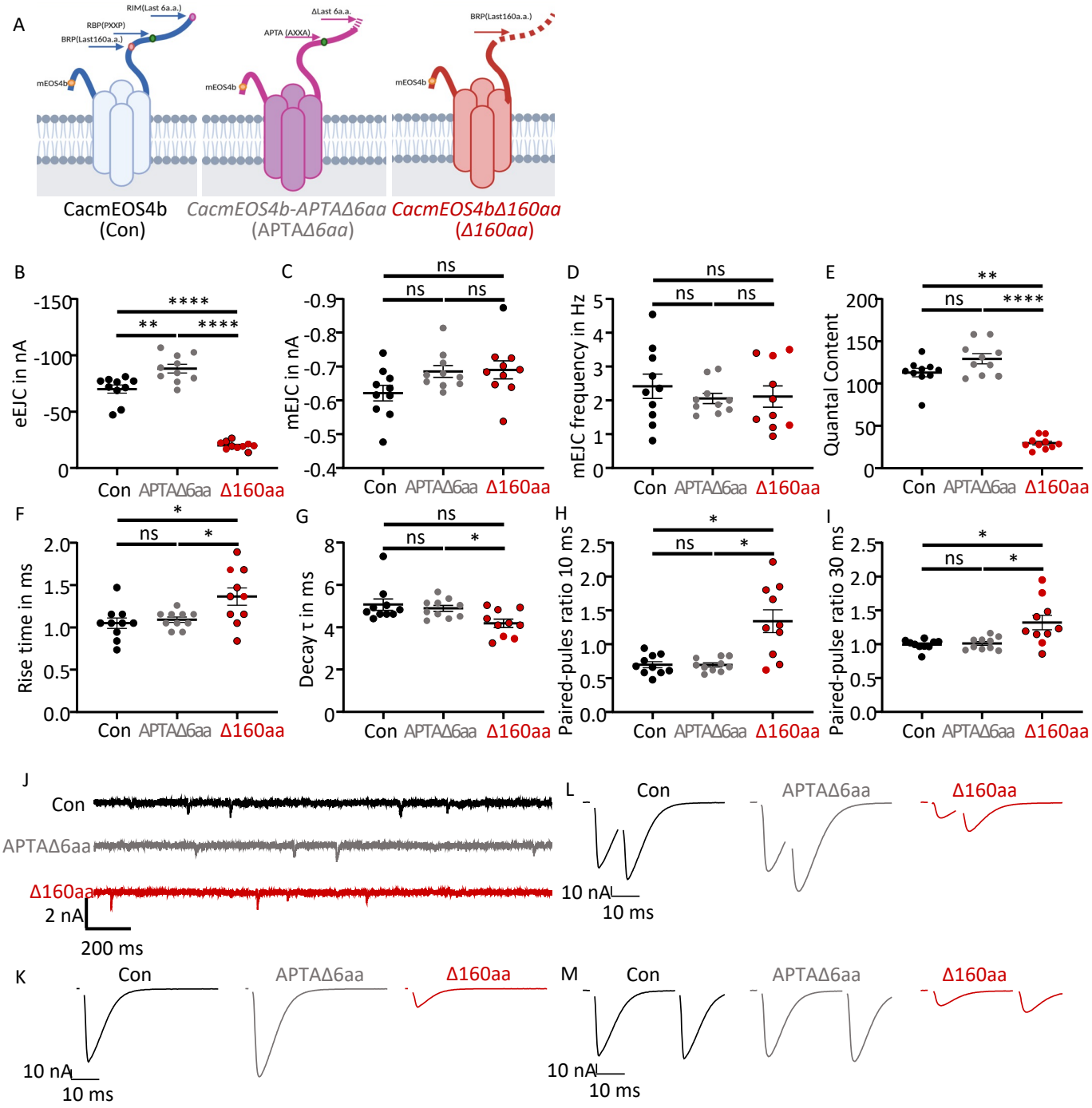

Figure S6. Electrophysiological characterization of Cac channels in *CacmEOS4B-APTAΔ6aa* and *CacmEOS4BΔ160aa* mutants. A) A Schematic diagram of on locus deletion mutants *CacmEOS4B-APTAΔ6aa* and *CacmEOS4BΔ160aa* animals generated from endogenously tagged CacmEOS4B control flies. (B-I) Electrophysiological recordings of *CacmEOS4B*, *CacmEOS4B-APTAΔ6aa* and *CacmEOS4BΔ160aa* animals using two-electrode voltage clamp (TEVC); quantifications for eEJC amplitude (B), mEJC amplitude (C) and mEJC frequency (D), Quantal content (E), eEJC rise time (F) and first order decay constant τ (G) and paired-pulse ratios (inter stimulus interval [ISI] of 10 ms (H) and 30 ms (I)). (J-M) Representative traces of mEJC (J), eEJC (K), 10 ms ISI (L) and 30 ms ISI (M) TEVC recordings. Measurements were performed at third-instar larval muscle 6 NMJs of abdominal segments 2 and 3.

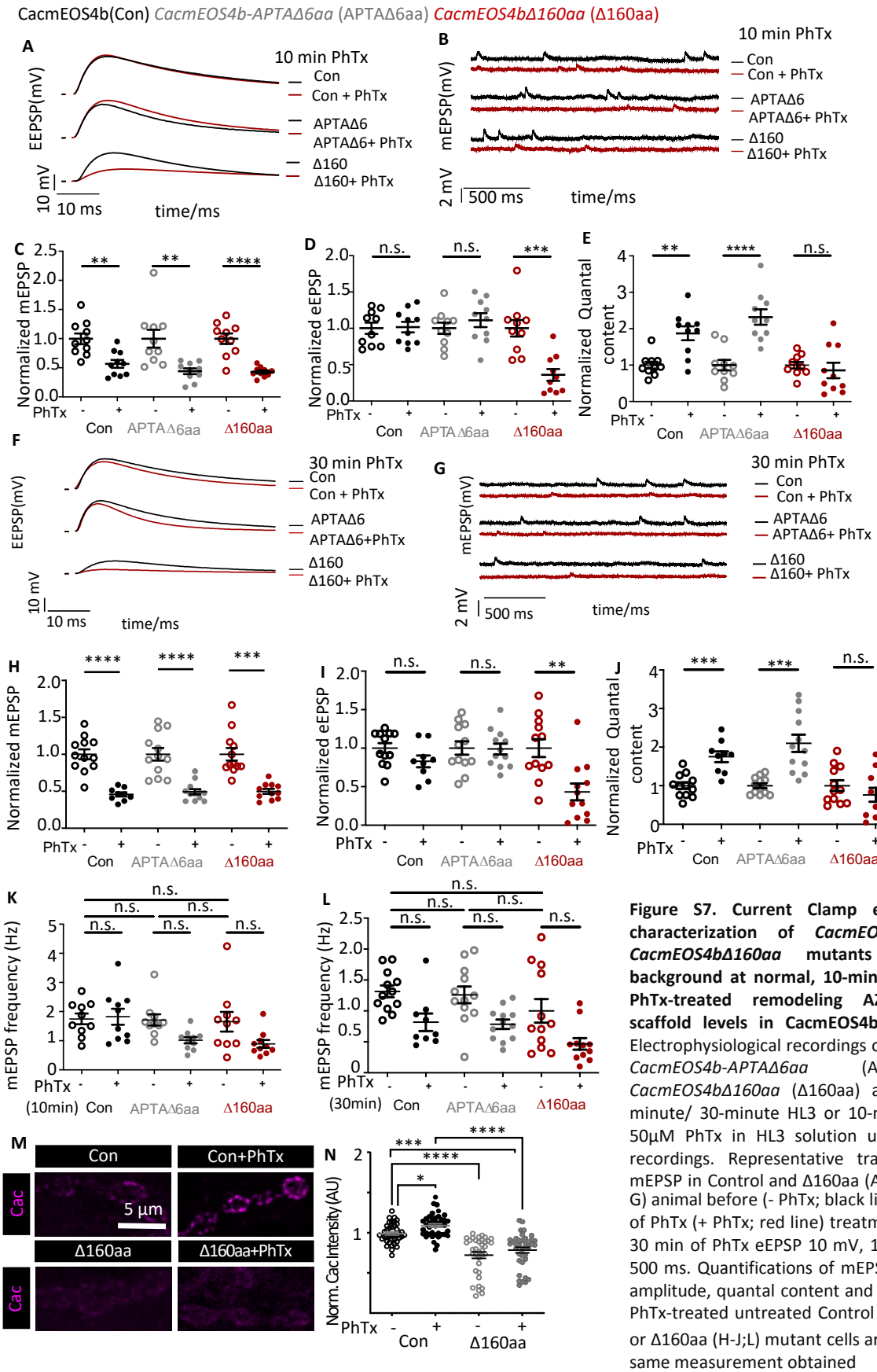

Figure S7. Current Clamp electrophysiological characterization of *CacmEOS4b-APTAΔ6aa* & *CacmEOS4bΔ160aa* mutants in CacmEOS4B background at normal, 10-minute and 30-minute PhTx-treated remodeling AZs and Confocal scaffold levels in CacmEOS4bΔ160aa mutants . Electrophysiological recordings of CacmEOS4B *(Con)*, *CacmEOS4b-APTAΔ6aa* (APTAΔ6aa) and *CacmEOS4bΔ160aa* (Δ160aa) animals after a 10-minute/ 30-minute HL3 or 10-minute / 30-minute 50µM PhTx in HL3 solution using current clamp recordings. Representative traces of eEPSP and mEPSP in Control and Δ160aa (A-B) or APTAΔ6aa (F-G) animal before (- PhTx; black line) and after 30 min of PhTx (+ PhTx; red line) treatment. Scale bar: after 30 min of PhTx eEPSP 10 mV, 10 ms; mEPSP 5 mV, 500 ms. Quantifications of mEPSP amplitude, eEPSP amplitude, quantal content and mEPSP frequency in PhTx-treated untreated Control and Δ160aa (C-E, K) or Δ160aa (H-J;L) mutant cells are normalized on the same measurement obtained without PhTx for each genotype. Measurements were performed at third-instar larval muscle 6 NMJs of abdominal segments 2 and 3. M-N, Representative confocal images of CacmEOS4B and *CacmEOS4BΔ160aa-/-* third instar larvae muscle4 NMJs subjected to 10-minute PhTx in HL3 or plain HL3 incubation, fixed and stained for Cac(purple). Quantification of Cac (N) intensity levels normalized to untreated control CacsfGFP images , N= 40 images, 4 sets. Data is represented as mean ± SEM. Data distribution is statistically tested by a one-way ANNOVA with a Dunn's multiple comparison test. Scale Bar= 5µm.

A		pGADT7	
		BRP	Control
pGBKT7	Cacophony C-term	+++++	-----
	Δ304 aa	-----	-----
	Δ130 aa	---++	-----
	Δ81 aa	---++	-----
	Δ60 aa	+++++	-----
human laminin C (aa 66-230)		-----	+++++

Figure S8. Cacophony C-terminal interaction surface harbors binding to RIM-1 and RBP protein binding sites. A) Yeast two hybrid assay of testing interaction between various Cac Channels constructs of its C-terminal with a BRP N-terminal construct. (A) A range of Cac C-terminal deletion constructs namely: -d304aa, -d130aa, d81aa, -d60aa, d31aa were used as prey constructs. A strong interaction was observed with N-terminal BRP-D1 fragment (amino acid position 1—320) construct as the prey and Cac C-term full-length construct, -d60aa and- d31aa baits. Interaction Legend: 5 clones were tested /double transformation; '-': no interaction ,'+': interaction. Positive control: pGADT7 SV40 large T-antigen (aa-84-708) vs. PGBKT7 Mouse p53 (aa72-390). Negative controls: PGBKT7 laminin and empty pGADT7 were used.

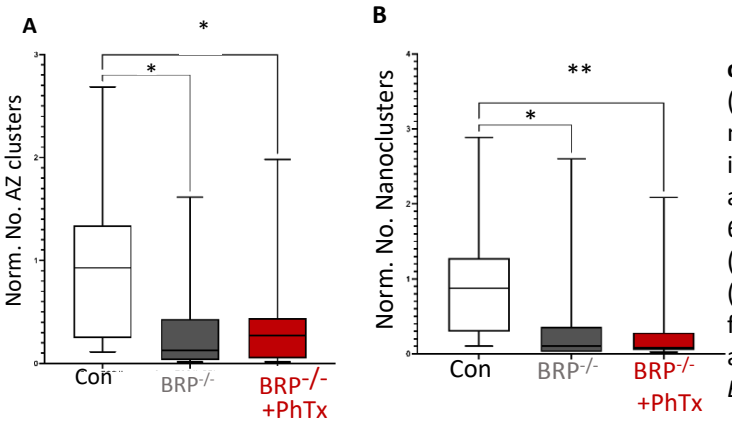

Figure S9. Cac channels in BRP$^{-/-}$ mutant AZs at normal or PhTx-treated remodeling AZs.
(A-B) Analysis from live sptPALM DATA depicting the number of Cac clusters identifiable with tessellation per image in CacmEOS4B (Con), *CacmEOS4B; BRP$^{-/-}$* (BRP$^{-/-}$) and *CacmEOS4B; BRP$^{-/-}$* after PhTx (BRP$^{-/-}$+PhTx) muscle 6/7 NMJs imaged and analyzed in Figure 5. N=30 ROIs (CacmEOS4B or Con), N=8 ROIs (BRP$^{-/-}$) and N=12 images (BRP$^{-/-}$) +PhTx) images were extracted from 3-4 animals for each condition yielding 72 AZ (control), 80 AZ (BRP$^{-/-}$), and 26 AZ (BRP$^{-/-}$ +PhTx) in the analysis, n=3 individual *BRP$^{-/-}$* experiments conducted with concurrent controls.

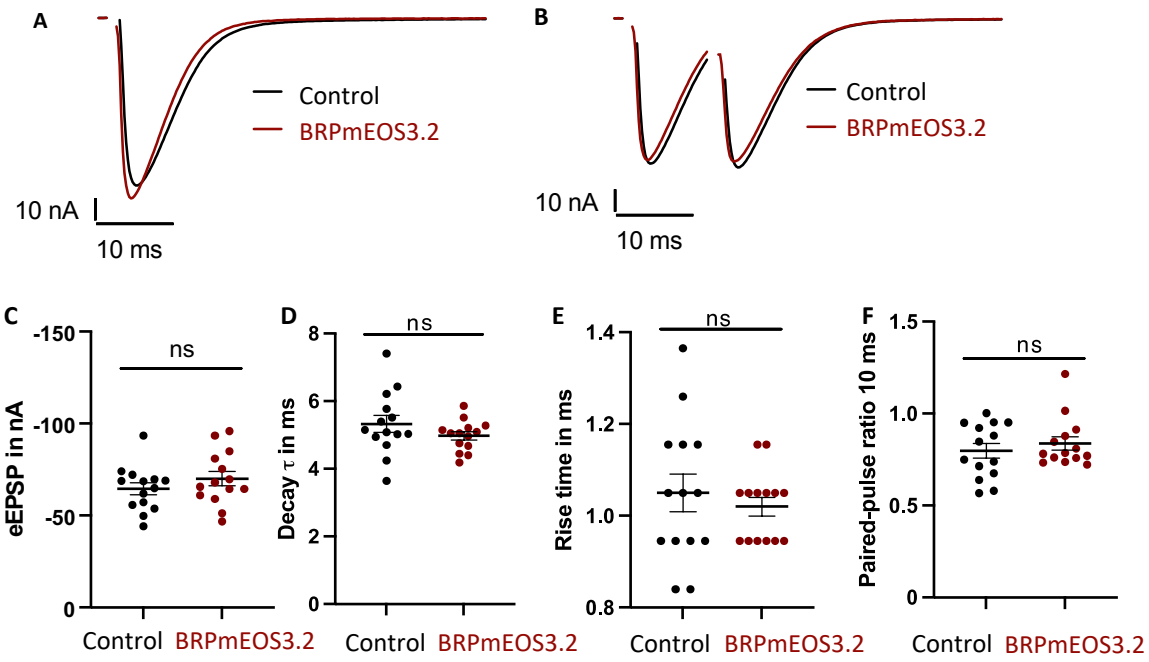

Figure S10. Electrophysiological characterization of Endogenously tagged BRPmEOS3.2 flies behave like control animals. Single copy of tagged BRPmEOS3.2 (BRPmOES3.2/BRP69) and single copy of endogenous BRP scaffold(BRP69/+ or Control) behave identically with two-electrode voltage clamp (TEVC) recordings. (A-D) Representative traces of eEPSP (A) and 10 ms ISI (B) TEVC recordings. Electrophysiological recordings of BRPmEOS3.2 and control animals using quantifications for eEPSP amplitude (C), first order decay constant τ (D), eEPSP rise time (E) , paired-pulse ratio (inter stimulus interval [ISI] of 10 ms (F). Measurements were performed at third-instar larval muscle 6 NMJs of abdominal segments 2 and 3.

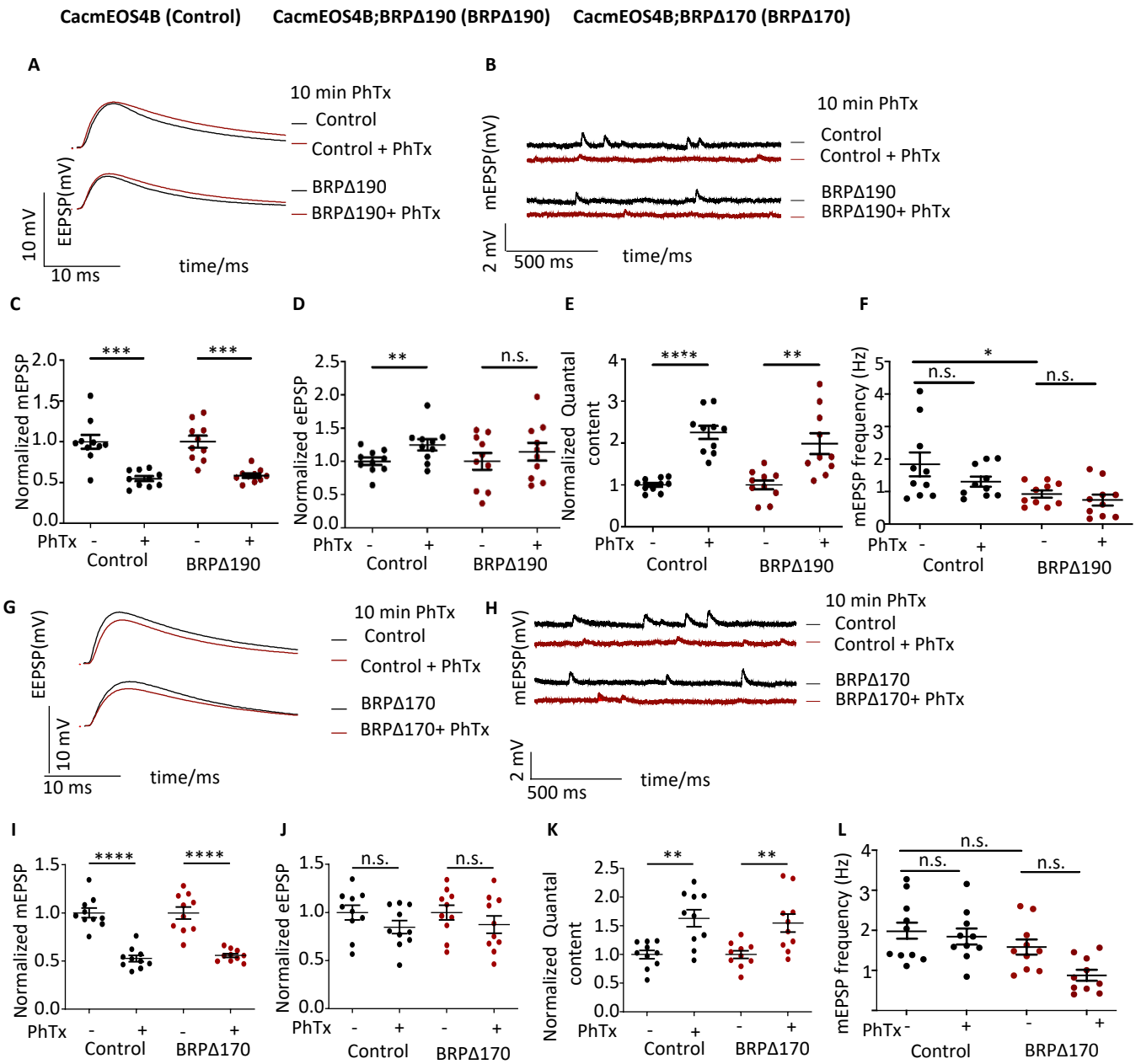

Figure S11. Electrophysiological characterization of BRPΔ170 and BRPΔ190 mutants in CacmEOS4B background at normal or 10-minute PhTx-treated remodeling AZs. Electrophysiological recordings of *CacmEOS4B* (Control), CacmEOS4B;BRPΔ170/brp69 (BRPΔ170) and CacmEOS4B;BRPΔ190/brp69(BRPΔ190) animals after a 10-minute HL3 or 10-minute 50μM PhTx in HL3 solution using current clamp recordings. Representative traces of eEPSP and mEPSP in Control and BRPΔ190 (A-B) or BRPΔ170 (G-H) animal before (- PhTx; black line) and after 30 min of PhTx (+ PhTx; red line) treatment. Scale bar: eEPSP 10 mV, 10 ms; mEPSP 5 mV, 500 ms. Quantifications of mEPSP amplitude, eEPSP amplitude, quantal content, and mEPSP frequency in PhTx-treated untreated Control and BRPΔ190 (C-F) or BRPΔ170 (I-L) mutant cells are normalized on the same measurement obtained without PhTx for each genotype. Measurements were performed at third-instar larval muscle 6 NMJs of abdominal segments 2 and 3.

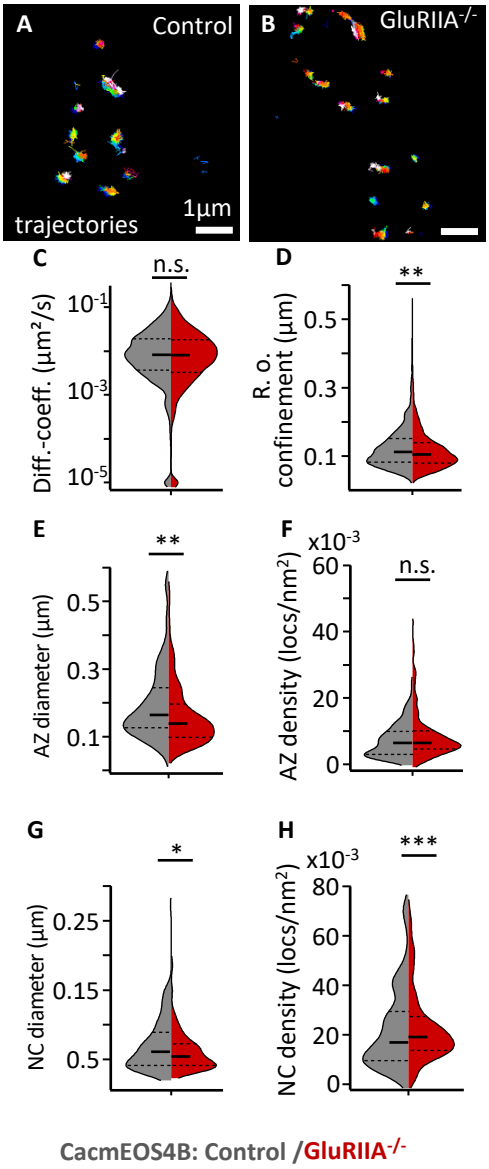

Figure S12. Cac channels in *GluRIIA* mutant AZs channel visualized for their live mobility and distribution at AZs. Live sptPALM imaging of *CacmEOS4B* (Control) and *CacmEOS4B;;GluRIIA*$^{-/-}$ mutants imaged in 1.5mM Ca^{2+} extracellular imaging buffer. Representative boutons displaying trajectory maps (A-B) Scale bar: (A-B): 1 µm. (C-D), live sptPALM diffusion coefficient and radius of confinement quantification of *CacmEOS4B* and *CacmEOS4B;;GluRIIA*$^{-/-}$ NMJs, N=19 (Con) and 20 (*GluRIIA*$^{-/-}$) ROIs from 10 animals respectively from which 3086 (Con) and 4100 GluRIIA$^{-/-}$) trajectories were analyzed. (E-H) Tessellation analysis of the diameter and density of Cac channels localizations within Nanocluster (NC) (G-H) and Active Zone (AZ) (E-F) boundaries from the same data as in C-D yielded 145 (Con) and 334 (GluRIIA$^{-/-}$) AZs that were analyzed. n=3 individual GluRIIA$^{-/-}$ *experiments were conducted with concurrent controls. PALM Data distribution was statistic*ally tested with Kolmogorov-Smirnov test. Statistical significance is denoted as asterisks: *p < 0.05; **p < 0.01; ***p < 0.001; ****p < 0.0001.

Supplemental Figure legends for Supplemental movies:

Supplemental Movie 1: Single molecule localization microscopy experiments in *Drosophila* larvae.
Representative movie of an entire Drosophila Muscle 6 NMJ imaged live, in vivo with sptPALM for 5000 frames at 20 Hz frame rate (1-2643 frames shown). This movies reflects the data shown in Figure S1A-C where (A), the PALM localization map (B) and trajectory map (C) derived from analysis of this movie.

Supplemental Movie 2: Activity during single molecule localization microscopy experiments in *Drosophila* larvae under low calcium. Live imaging of third-instar larvae at muscle 4 of *CacmEOS4b;;Syn-GCAMP6f* first imaged in low calcium (0.2 mM Ca^{2+}) extracellular imaging solution Supplemental Movie 2 references data in Figure S3A-E. Here a live Syn-GCAMP6f recording was performed for 5000 frames at 50 Hz (Fig. S3C-E), and an accumulated activity masks of (Fig. S3C) are shown in (Fig. S3D and S3E). Following this imaging a sptPALM recording of CacmEOS4b was performed at 20 Hz for 5000 frames (Fig. S3A-B).

Supplemental Movie 3: Activity during single molecule localization microscopy experiments in *Drosophila* larvae under 1.5mM **calcium.** Live imaging of the same third-instar larvae and the same muscle 4 of *CacmEOS4b;;Syn-GCAMP6f* imaged in Supplemental Movie 2 references data in control (1.5 mM Ca^{2+}) extracellular imaging solution and analysed in Figure S3F-J. Here again, a live Syn-GCAMP6f recording was performed for 5000 frames at 50 Hz (Fig. S3H-J), and an accumulated activity masks of (Fig. S3H) are shown in (Fig. S3J and S3I), respectively. Following this imaging a sptPALM recording of CacmEOS4b was performed at 20 Hz for 5000 frames (Fig. S3F-G).